

1

2 **Supplementary information (SI) for:**

3

4 Adaptive laboratory evolution and independent component analysis
5 disentangle complex vancomycin adaptation trajectories

6

7 ¹Anaëlle Fait*, ^{2,3}Yara Seif*, ¹Kasper Mikkelsen, ²Saugat Poudel, ⁴Jerry M. Wells, ²Bernhard O.
8 Palsson, ¹Hanne Ingmer[†]

9

10 ¹ University of Copenhagen, Department of Veterinary and Animal Sciences, Food safety and
11 zoonosis, Stigbøjlen 4, 1870 Frederiksberg, Denmark

12 ² Department of Bioengineering, University of California, San Diego, La Jolla, CA, 92093, USA

13 ³ Merck & Co., Inc., South San Francisco, CA 94080, USA

14 ⁴ Host-Microbe Interactomics, Animal Sciences Group, Wageningen University, De Elst 1,
15 Wageningen, The Netherlands

16

17 [†]Hanne Ingmer

18 *A.F. and Y.S. contributed equally to this study

19

20 **Email:** hi@sund.ku.dk

21 **SI Materials and Methods:**

22

23 **Serial transfer experiments.** The MRSA strain JE2, a plasmid-cured derivative of USA300 LAC,
24 was grown on increasing concentrations of vancomycin in tryptic soy broth medium (TSB) using a
25 two-step protocol derived from Rodriguez de Evgrafov *et al.* 2015 (1) (**Figure S6**). In the first step,
26 the bacteria were challenged with increasing concentrations of vancomycin. Overnight cultures
27 were diluted to 10^5 CFU/ml and used to inoculate a microtiter plate containing 0.25 to 0.5µg/ml
28 increments in vancomycin concentration. After 18h at 37°C in a fixed incubator, the plates were
29 visually inspected for growth. The highest concentration to which JE2 grew (subMIC) was recorded,
30 and this culture was used to inoculate fresh TSB media supplemented with vancomycin at the
31 strains subMIC and allowed to grow overnight in 3mL cultures. This second step was used to
32 stabilize any adaptive event occurring from the previous challenge. This two-step evolution
33 procedure is referred to as an Exposure cycle (E). The culture was used to start a new cycle, and
34 an aliquot was saved in glycerol at -80°C. 10 independent cultures were grown in parallel resulting
35 in the lineages L1 to L10. This process was repeated for 30 exposure cycles (60 days) and thorough
36 characterization was conducted every 10 cycles at timepoints E10, E20 and E30. L5_E20 and
37 L9_E20 were re-adapted to vancomycin for 10 cycles resulting in the 2 additional clones L5_E30bis
38 and L9_E30bis. L3_E20 contaminated a parallel culture during the laboratory evolution resulting in
39 two E30 strains for the same lineage, L3_E30 and L3_E30bis. The cultures were regularly plated
40 on TSA to visually check for contaminants.

41

42 **Genome Sequencing and Mutation Analysis.** DNA sequencing was performed on the JE2 strain,
43 and the JE2-derived vancomycin adapted clones. Chromosomal DNA was isolated using the
44 DNeasy Blood & Tissue Kit (Qiagen) and concentrations were normalized using a Qubit
45 (Invitrogen). Sequencing libraries were prepared using the Nextera XT DNA sample preparation kit
46 (Illumina). Paired-end sequencing was performed at Statens Serum Institut in Copenhagen using
47 the NextSeq 550 system (Illumina). Data analysis was performed in CLC Genomics Workbench
48 version 8.0. Reads were mapped against the *S. aureus* USA300_FPR3757 reference genome

49 (Genbank accession no. NC_07793). The frequency cut-off for variant calling was set at 30% and
50 all the detected mutations were verified manually to ensure homogeneity of the variants across
51 reads and avoid false detection due to imperfect mapping. The variants identified during alignment
52 of JE2 to the *S. aureus* USA300_FPR3757 reference genome were excluded in the variant call for
53 vancomycin-adapted clones. Detailed information on variant calling is presented in **Dataset S1**. We
54 verified that the passaged populations were homogeneous by sequencing the whole population for
55 L9 at E20 in addition to sequencing the single clone L9_E20. There were no additional mutations
56 during sequencing of the L9 population compared to the single clone, suggesting that the
57 populations are homogeneous (**Table S9**). However, we detected an additional mutation in the
58 single clone L9_E20 that was not present in sequencing of the whole population, or in sequencing
59 of the subsequent isolate L9_E30, which suggests that the additional mutation in L9_E20 was
60 acquired during isolation of the single clone from the population prior to sequencing. The mutation
61 is a synonymous mutation in the gene *relA*.

62

63 **Construction of plasmids and strains.** All plasmid constructs were cloned in *E. coli* IM08B (2)
64 then transformed into *S. aureus* strain JE2. For expression of *vraX*, SAUSA300_RS02980,
65 SAUSA300_RS08750, *sceD*, *vraR*, *vraS*, *vraT* and *vraU*, the genes including their predicted
66 ribosomal binding site were cloned into the Sall and EcoRI sites of pSK9067 behind the IPTG-
67 inducible P_{spac} promoter (3) using primer pairs listed in **Table S10**, concurrently removing the *gfp*
68 reporter gene. The *vraT* and *walk* mutants were obtained by genetic recombination using the
69 protocol by Monk and Stinear, 2021 (4). The *vraT* mutations present in clones L7_E30, L8_E20
70 and L10_E20 were amplified with 700bp flanking sequences. Due to gene essentiality, the entire
71 sequence of *walk* was amplified with equal-sized flanking regions upstream and downstream of
72 the mutations present in clones L1_E20 and L7_E20. The inserts were cloned into pIMAY-Z
73 backbone using the SLiCE (Seamless Ligation Cloning Extract) ligation extract. After pIMAY-Z
74 integration and plasmid excision, putative mutants were screened by sequencing.

75

76

77 **Mutation co-occurrence analysis.** To assess the co-occurrence of mutations across strains, we
78 built a weighted graph in Networkx in which mutations were represented as nodes and co-
79 occurrence of two mutations in strains were represented by edges. To inspect the chronology of
80 mutation emergence, we constructed two separate weighted undirected graphs for each exposure
81 level. The first graph accounted for mutations arising at E20 across 10 clones (L1 through L10),
82 while the second graph accounted for mutations arising at E30 across 12 clones (L1 through L10,
83 L3bis, L5bis and L9bis). Edges were weighted according to the reciprocal of the number of times
84 two mutations co-occurred in the same strain. The Girvan-Newman method was then used to find
85 communities in the graph. Communities are defined as a subset of nodes that share a significantly
86 larger number of connections than with the rest of the network (5). In this specific case, communities
87 represent sets of mutated loci that have a higher co-occurrence frequency. Thus, communities
88 capture potential mutational trajectories at E20 and E30. Next, to represent the importance of a
89 mutated locus within its community we calculated the harmonic centrality of each node. The
90 harmonic centrality is described as the sum of the reciprocal of the shortest path distances $d(v, u)$
91 from all other nodes to node u .

92

$$93 \quad C(u) = \sum_{v \neq u} \frac{1}{d(v,u)} \quad \text{Eq (1)}$$

94 In other words, a mutated locus is more central when it occurs across a larger number of clones
95 and co-occurs with a larger number of nodes and is therefore more closely connected to all other
96 nodes. We proceeded to compute the edge betweenness centrality, which is a measure of the
97 importance of an edge in a graph. Mathematically, it is described as the fraction of shortest paths
98 $\sigma(s, t)$ in a graph that include edge e and is calculated for all edges.

99

$$100 \quad C_B(e) = \sum_{s,t \in V} \frac{\sigma(s,t|e)}{\sigma(s,t)} \quad \text{Eq (2)}$$

101

102 To highlight nodes and edges that significantly skew the distribution of computed centralities, we
103 iteratively removed nodes and edges and re-computed centrality values for each sub-network. We

104 then ran a normality test for each z-scored distribution and highlighted the nodes/edges for which
105 the p-value dropped below 0.05.

106

107 **Independent Component Analysis of transcriptomic profile.** RNA-sequencing and ICA pipeline
108 used to calculate iModulon structure and activities have been in described in full detail in previous
109 publications (6, 7). Here, normalized transcripts per million (TPM) from 33 new RNA-seq profiles
110 were calculated concatenated to the previously published 108 profiles (7). The combined dataset
111 was centered to strain-specific reference conditions. These conditions are labeled
112 “USA300_TCH1516_U01-Set000_CAMHB_Control_1”, “USA300_TCH1516_U01-
113 Set000_CAMHB_Control_2” for TCH1516; and “USA300_LAC_U01-Set001_CAMHB_Control_1”,
114 “USA300_LAC_U01-Set001_CAMHB_Control_2” for LAC. The combined centered dataset was
115 used for ICA decomposition with 100 iterations, and 10e-8 tolerance and 46 components.

116

117 ICA outputs an $\mathbf{S}_{(\text{genes} \times \text{IC})}$ and an $\mathbf{A}_{(\text{components} \times \text{samples})}$ matrix, corresponding to structure and activity
118 of iModulons, respectively. The $\mathbf{S}_{(\text{genes} \times \text{IC})}$ matrix lists the weights of each gene (rows) in each
119 extracted component (columns). Most gene weightings in each of the independent components of
120 \mathbf{S} are normally distributed. However, weightings of genes in an iModulon, representing the signal
121 for each component fall outside this normal distribution, i.e. the absolute value of their weights are
122 higher than what would be expected of a normally distributed variable (6). To enrich these genes,
123 we used Scikit-learn’s implementation of the D’Agostino K2 test, which measures the ‘normality’ of
124 sample distribution based on skew and kurtosis (8, 9). For each component in \mathbf{S} , weights were
125 converted to their absolute value, and genes were sorted by the absolute weightings in that
126 component. Genes with the highest weighting were then removed iteratively until the D’Agostino
127 K2 test for the remaining distribution fell below the previously tested cutoff value of 280. The outlier
128 genes which were removed constitute the gene set of an iModulon.

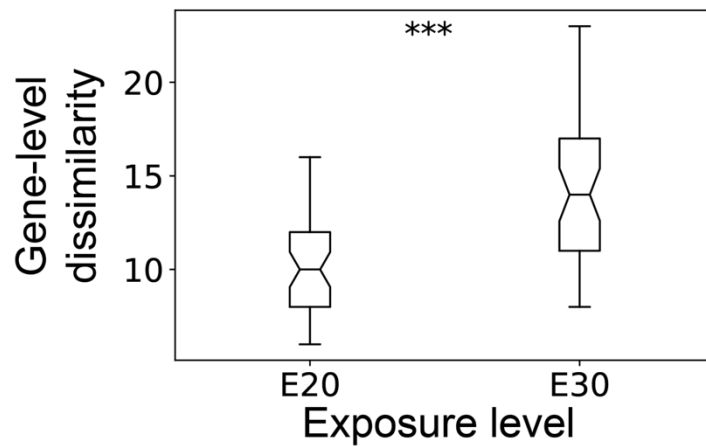
129

130 The analysis yielded 40 robust independent components (IC, **Dataset S2**). We proceeded to
131 annotate the 40 iModulons with biological annotations. As a first step we compared each iModulon

132 to assembled and curated annotations containing features such as known regulons, genomic
133 islands, prophages etc (7). Next, we mapped each iModulon to a regulon by either comparing
134 iModulon gene sets to differentially expressed genes in transcription factor knockout experiments
135 or by implementing the RegPrecise algorithm (10–14). The iModulon genes for each component
136 were compared to this database for significant overlap using Fisher's exact test with FDR of 0.05.
137 If iModulon genes had any significant overlap with the features in the dataset with precision ≥ 0.5
138 and recall ≥ 0.2 , the iModulon was annotated with the feature name e.g. VraR, ϕ Sa3, CcpA etc.
139
140

141 **SI Figures:**

142



143

144 **Figure S1: Mutational divergence indicated by increasing gene-level mutation dissimilarity**

145 **across exposure levels.** We compared the pairwise dissimilarity in the identity of mutated genes

146 across exposure levels. On average, two clones differ by 9.7 +/-2.7 mutated genes at E20, and by

147 14.2 +/- 3.5 mutated genes at E30. A Student's t-test underscores a significance increase in

148 dissimilarity in mutational profiles across evolutionary time ($p \ll 0.01$, statistic = -6.8). N.b., we

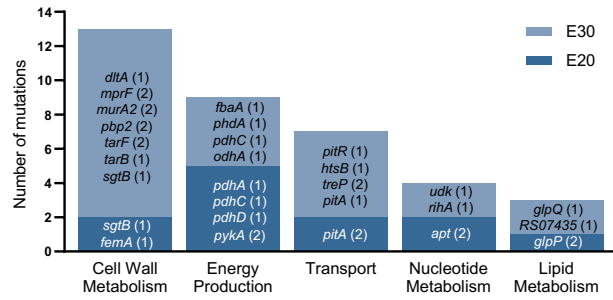
149 excluded L3_E30, L5_E30 and L9_E30 profiles from our analysis, for the benefit of correctly

150 accounting for mutations accumulated across L3_E30bis, L5_E30bis, and L9_E30bis, respectively,

151 and to avoid the bias resulting from high similarity between replicate pairs.

152

153

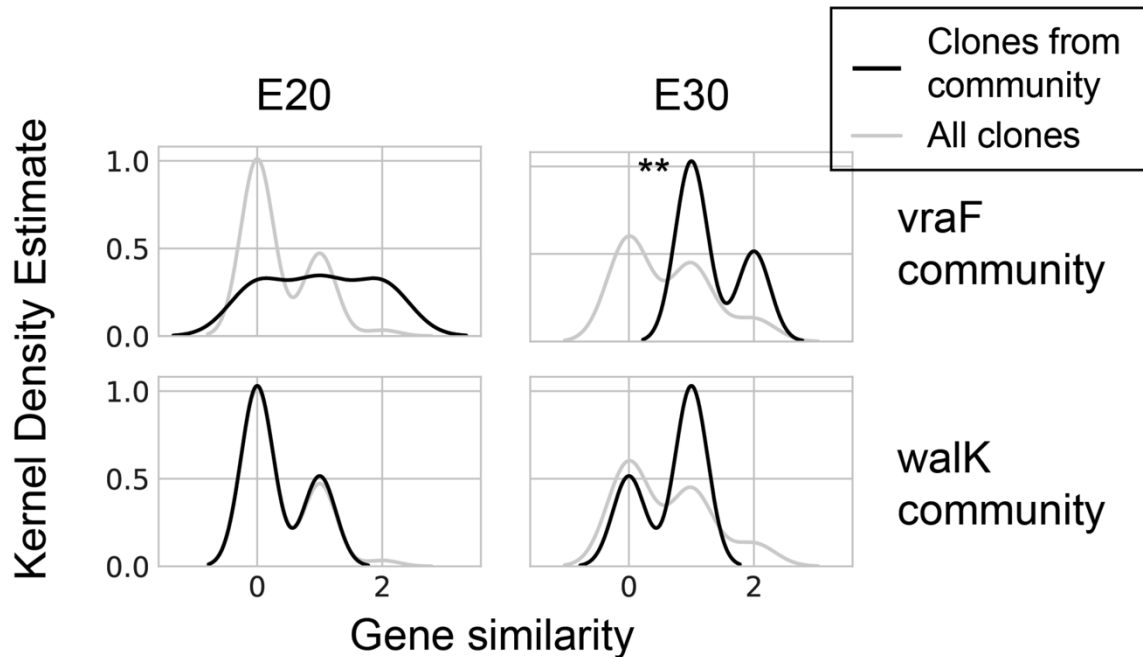


154

155 **Figure S2. Mutations in metabolism COG subsystems at E20 and E30.** The mutated genes in
 156 each COG subsystem are presented in each graph bar. The number of times the gene was
 157 mutated across lineages is shown in parentheses.

158

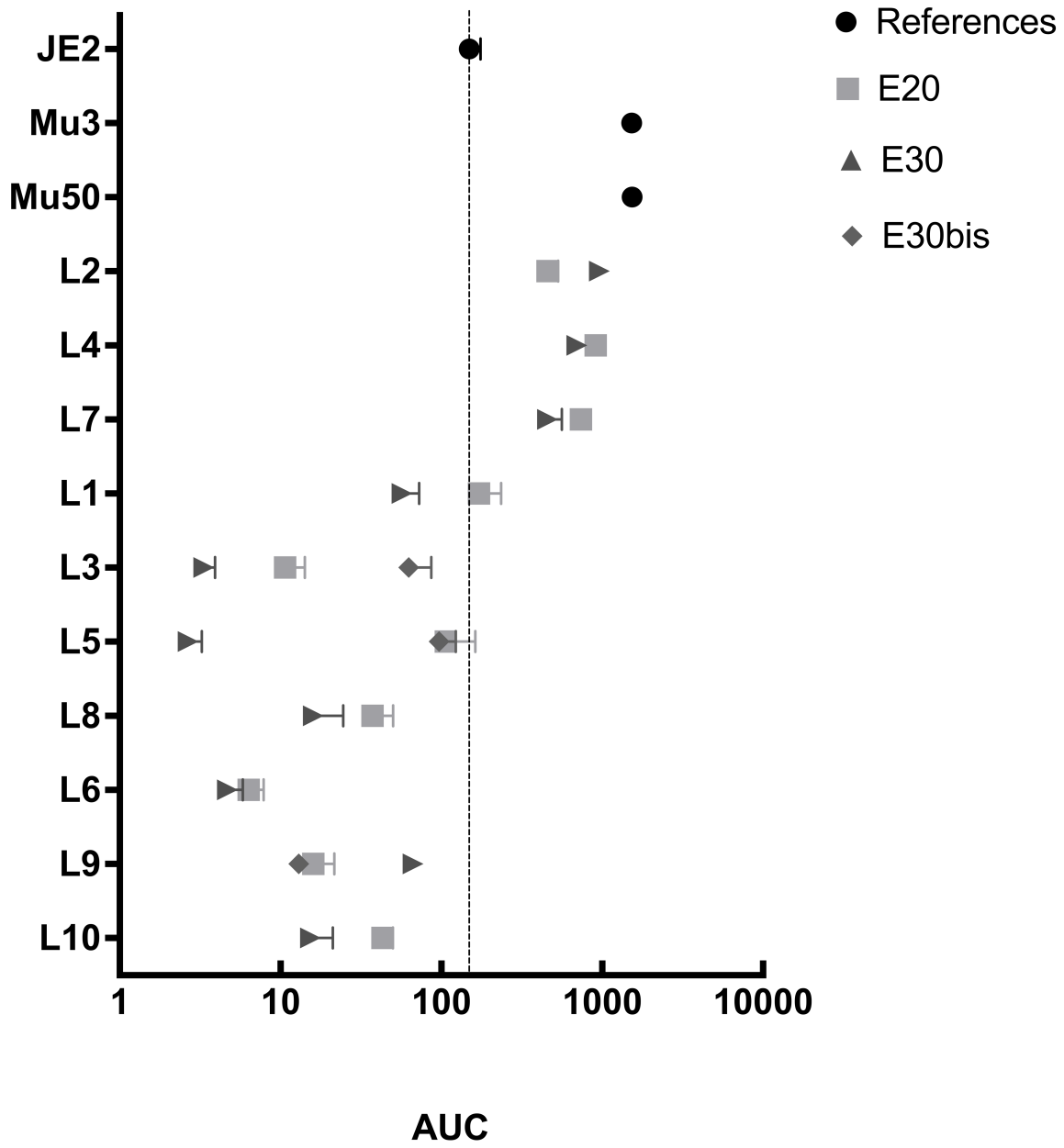
159



160

161 **Figure S3: Gene level similarity across sub-communities of clones identified through**
 162 **network analysis of mutational patterns.** We compare the gene level similarity (pairwise
 163 number of shared mutated genes) across the two sub-communities (in black, *vraF*: L2, L5 and L6,
 164 and *walk*: L4, L7 and L8) in comparison to the background (in grey, all strains) across exposure
 165 levels. Interestingly, we notice that while at E20, gene level similarities within the two sub-
 166 communities are comparable to background, the distribution is right shifted at E30, with a larger
 167 number of common genes being target by mutations within the respective sub-communities than
 168 in the background population. On average, two clones of the *walk* sub-community share 1.3
 169 mutated genes (in contrast to only 0.6 for two random clones), while two clones from the *vraF*
 170 community share 0.66 mutated genes. We observe statistical significance for the *walk*
 171 community.

172



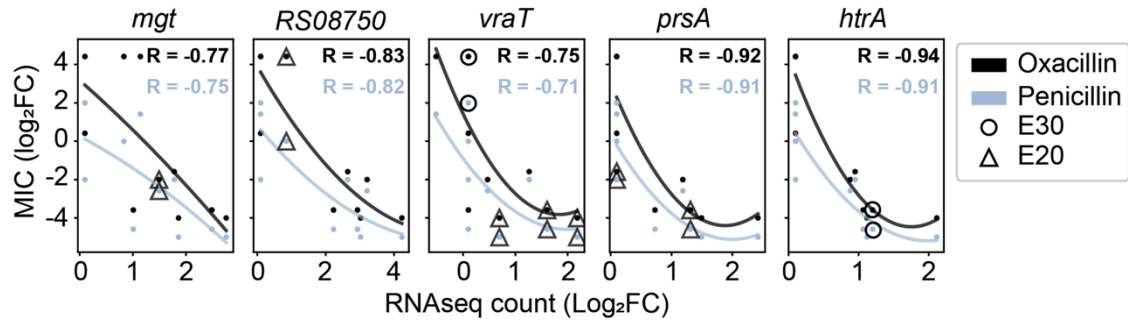
173

174 **Figure S4. Oxacillin susceptibility of JE2-derived VISA strains by PAP-AUC.** Each datapoint

175 shows the mean AUC for 3 to 6 biological replicates. The error bars represent standard

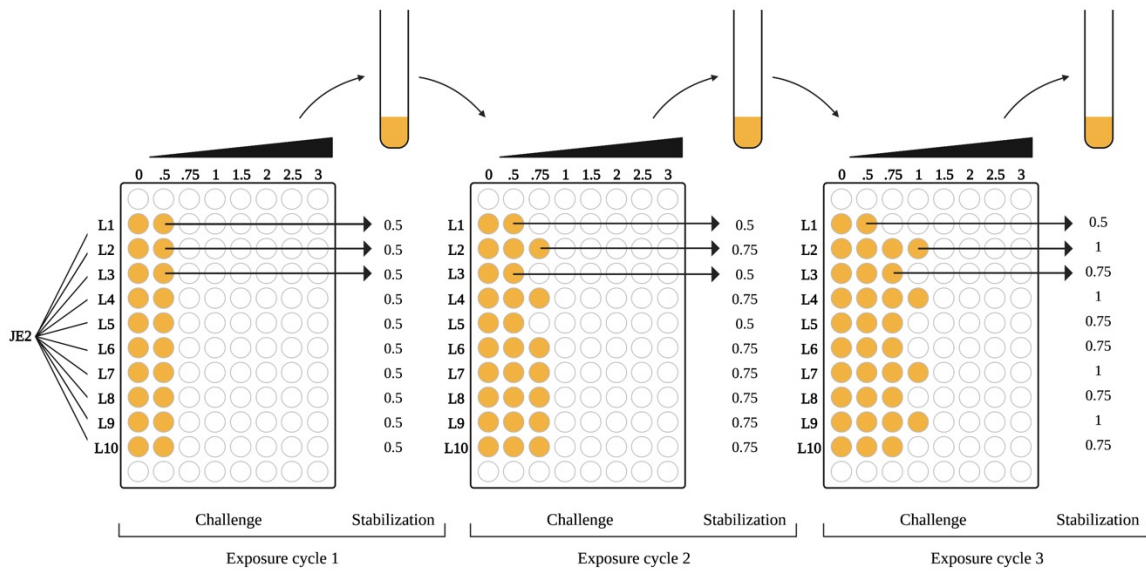
176 deviations.

177



178

179 **Figure S5. Correlation between transcriptional profile of vancomycin-adapted strains and**
 180 **antibiotic susceptibility.** Correlation between gene expression and antibiotic susceptibility (each
 181 dot represents a clone, triangles are traced around the dots if the clone is mutated for that gene,
 182 blue: penicillin, black: oxacillin.



183

184 **Figure S6. Illustration of vancomycin adaptive laboratory evolution.** The MRSA strain JE2 was

185 inoculated in 10 parallel cultures and adapted to vancomycin following a two-step protocol. In the

186 first step, the cultures were challenged with increasing concentrations of vancomycin in 96-well

187 plates. The plates were incubated at 37°C overnight. Aliquots from the highest concentration where

188 growth was observed was used to inoculate tubes containing fresh media and sub-inhibitory

189 concentrations of vancomycin. This second step was used to stabilize any possible adaptation from

190 the vancomycin challenge. The cultures were incubated at 37°C overnight and used to start a new

191 exposure cycle. Yellow coloring represents bacterial growth.

192 **SI Tables:**

193

194 **Table S1. Phenotypic characterization of vancomycin adapted JE2 clones at timepoints E10,**

195 **E20 and E30.** Doubling time expressed in minutes. Vancomycin and oxacillin susceptibility tested

196 using population analysis profile – area under the curve (PAP-AUC).

	Doubling time (min)				PAP-AUC Vancomycin (ratio to Mu3)				PAP-AUC Oxacillin (AUC)			
	E10	E20	E30	E30bis	E10	E20	E30	E30bis	E10	E20	E30	E30bis
JE2 (MRSA, ancestor)	31				0.6				149			
Mu3 (hVISA)	34				1				1528			
Mu50 (VISA)	45				3.04				1535			
L1	35	40	41		0.89	1.07	1.77		177	171	57	
L2	39	43	46		1.42	1.86	2.45		559	457	962	
L3	35	38	45	54	1.02	1.19	2.15	2.42	17	11	3	63
L4	35	47	51		1.41	1.88	2.74		97	910	694	
L5	38	38	44	41	1.00	1.20	2.39	1.45	103	106	3	97
L6	37	48	51		0.90	1.65	1.69		111	6	5	
L7	32	37	40		0.87	1.22	2.04		263	738	457	
L8	37	44	48		1.20	2.42	3.16		50	37	16	
L9	34	41	44	47	1.22	2.47	2.88	3.07	160	16	67	13
L10	35	38	42		1.34	1.40	2.15		63	43	15	

197

198 **Table S2. Type of mutations from sequencing timepoint E20 and E30 of *in vitro***
199 **vancomycin evolved strains.** ORF: Open reading frame; SNP: Single nucleotide polymorphism.

	Mutations	Intergenic	ORFs	InDels	SNPs	Synonymous	Frameshift	Stop codon
E20	64	9	55	17	47	3	10	4
E30	109	11	98	25	84	3	13	5

200

201 **Table S3. Most mutated genes in JE2-derived hVISA and VISA lineages.** Genes/adjacent
 202 genes/operons mutated in more than one lineage. Bold: mutations in E30 not present in E20;
 203 underlined: mutations in E20 not present in E30.

Gene	Locus	Lineages mutated			
<i>vraT</i>	SAUSA300_RS10195	L8	L9	L10	L7
/	SAUSA300_RS04225	L1	L5	L2	L10
<i>graS</i>	SAUSA300_RS03465	L1	L3bis		
<i>vraF</i>	SAUSA300_RS03470	L9	L3	L5	L10
<i>vraG</i>	SAUSA300_RS03475	L7			
<i>pitR</i>	SAUSA300_RS03480	L4			
<i>pitA</i>	SAUSA300_RS03485	L4	L8	L3	
<i>ssaA</i>	SAUSA300_RS12415	L3	L5	L10	
autolysin	SAUSA300_RS09395	L3	L6	L9	
<i>walkR</i>	SAUSA300_RS00110	L4	L7	L1	
	SAUSA300_RS00105	L8			
	SAUSA300_RS00115	L8			
<i>rpoB</i>	SAUSA300_RS02820	L6			
<i>rpoC</i>	SAUSA300_RS02825	L2	L9		
<i>rpoD</i>	SAUSA300_RS08300	L2			
<i>pdhC</i>	SAUSA300_RS05360	L6	L3		
<i>pdhA</i>	SAUSA300_RS05350	L5			
<i>pdhD</i>	SAUSA300_RS05365	<u>L8</u>			
<i>puuR</i>	SAUSA300_RS05375	<u>L5</u>			
<i>pykA</i>	SAUSA300_RS08975	<u>L4</u>	<u>L7</u>		
<i>apt</i>	SAUSA300_RS08670	L1	L10		
<i>mprF</i>	SAUSA300_RS06820	L4	L8		
<i>rseP</i>	SAUSA300_RS06255	L2	L6		
<i>pbp2</i>	SAUSA300_RS07315	L1	L9		
<i>prsA</i>	SAUSA300_RS09800	L3	L9		
<i>tarF</i>	SAUSA300_RS01325	L8	L9		
<i>murA</i>	SAUSA300_RS11440	L7			
<i>fbaA</i>	SAUSA300_RS11445	L6			

204

205

206 **Table S4. TCS associated genes mutated in E20 and E30.** We investigated the mutations which
 207 were classified under cellular processes and signaling. We focused on the set of core *S. aureus*
 208 two-component systems (15), and collected recently determined regulons for each of eight two-
 209 component systems.

Regulator	Locus tag	Name	E20	E30
<i>vraRST</i>	SAUSA300_RS10135	<i>mgt</i>	1	2
	SAUSA300_RS08750	/	1	1
	SAUSA300_RS11440	<i>murA2</i>	0	1
	SAUSA300_RS09800	<i>prsA</i>	2	4
	SAUSA300_RS10195	<i>vraT</i>	4	7
<i>saeRS</i>	SAUSA300_RS12415	<i>ssaA</i>	4	7
<i>walKR</i>	SAUSA300_RS00105	<i>walR</i>	1	1
	SAUSA300_RS09395	autolysin	2	4
	SAUSA300_RS05375	<i>puuR</i>	1	2
	SAUSA300_RS09800	<i>prsA</i>	2	4
	SAUSA300_RS12415	<i>ssaA</i>	4	7
	SAUSA300_RS08750	/	1	1
	SAUSA300_RS00110	<i>walK</i>	3	3
	SAUSA300_RS10500	MAP domain	0	1
<i>graSR</i>	SAUSA300_RS03475	<i>vraG</i>	0	1
	SAUSA300_RS00105	<i>walR</i>	1	1
	SAUSA300_RS06255	<i>rseP</i>	2	2
	SAUSA300_RS10590	phiNM3(p)	0	1
	SAUSA300_RS04515	<i>dltA</i>	0	1
	SAUSA300_RS03470	<i>vraF</i>	1	5
	SAUSA300_RS02925	<i>sdrE</i>	0	1
	SAUSA300_RS02625	<i>ftsH</i>	0	1
	SAUSA300_RS03465	<i>graS</i>	0	2
	SAUSA300_RS01170	<i>glpQ</i>	0	1
	SAUSA300_RS06890	<i>femA</i>	1	1
<i>nreABC</i>	SAUSA300_RS03665	<i>fruR</i>	1	1
<i>sarA</i>	SAUSA300_RS03665	<i>fruR</i>	1	1
<i>lytSR</i>	SAUSA300_RS02825	<i>rpoC</i>	2	3
	SAUSA300_RS02820	<i>rpoB</i>	1	1
	SAUSA300_RS07105	<i>odhA</i>	0	1
	SAUSA300_RS06375	<i>rny</i>	1	2
	SAUSA300_RS05520	<i>ylbN</i>	0	1
<i>arlRS</i>	SAUSA300_RS06375	<i>rny</i>	1	2
	SAUSA300_RS12570	/	0	1
	SAUSA300_RS11315	<i>murA2</i>	0	1

210

211

212 **Table S5. Communities extracted from two co-occurrence graphs constructed at E20 and**
 213 **E30.** Genes included are targeted by a mutation in at least one clone.

	E20	E30
<i>Walk community</i>	<i>pdhD, walk, pitR, pitA, SAUSA300_RS13540, SAUSA300_RS10925, walR, glpP, vraT, SMSAP5(p1), SAUSA300_RS06395, SAUSA300_RS09680, stp1, fruR, rsbW, dnaQ, pykA</i>	<i>pitA, TarF_1, walR, glpP, SMSAP5(p1), PepSY domain p1, SAUSA300_RS09680, dnaQ, vraG, vraT, stp1, fruR, walk, tcaR, SAUSA300_RS10925, ebh, SAUSA300_RS06395, pykA, pdhD, SAUSA300_RS13540, yqfL, mprF, murA2, pitR, rsbW</i>
<i>VraF community</i>	<i>vraF, rny, puuR, SAUSA300_RS04225, rpoC, gdpP, ysdC, relA, apt, prsA, ssaA, sgtB, SAUSA300_RS11565, sagB, SAUSA300_RS08750, pdhC, rpoD, pdhA, rpoB, mfd, rseP, femA</i>	<i>SAUSA300_RS03100, vraF, rny, puuR, rihA, SAUSA300_RS04225, ylbN, SAUSA300_RS05040, rpoC, gdpP, SAUSA300_RS08675, fbaA, ysdC, relA, apt, prsA, SAUSA300_RS08095, graS, ssaA, odhA, sgtB, sdrE, pbp2, sagB, SAUSA300_RS11565, T2SS, SAUSA300_RS08750, rpoD, pdhC, rlmH, pdhA, rpoB, mfd, rseP, femA, TsaD, dltA</i>
<i>Walk community</i>	L1_E20, L10_E20, L4_E20, L9_E20, L7_E20, L8_E20	L9_E30bis, L7_E30, L3_E30, L8_E30, L10_E30, L4_E30, L1_E30
<i>VraF community</i>	L2_E20, L3_E20, L1_E20, L10_E20, L6_E20, L9_E20, L5_E20	L9_E30bis, L2_E30, L6_E30, L3_E30, L5_E30, L5_E30bis, L10_E30, L3_E30bis, L1_E30

214

215

216 **Table S6. Effect of vancomycin-adaptive *vraT* and *walk* mutations on vancomycin and**
 217 **oxacillin susceptibility.** Mutations in *vraT* and *walk* were amplified from JE2-derived VISA
 218 isolates (L7_E30, L8_E20, L10_E20, L1_E20 and L7_E20) and inserted into the chromosome of
 219 WT strain JE2. Vancomycin and oxacillin MIC was determined using Etests.

	Vancomycin MIC (mg/L)	Oxacillin MIC (mg/L)
JE2	0.75	16
JE2 <i>vraT</i> _{L7_E30}	1	256
JE2 <i>vraT</i> _{L8_E20}	1.5	256
JE2 <i>vraT</i> _{L10_E20}	1	256
JE2 <i>walk</i> _{L1_E20}	1	1
JE2 <i>walk</i> _{L7_E20}	1	1.5

220

221 **Table S7. Overexpression of selected genes in MRSA strain JE2.** Genes were cloned in
 222 plasmid pSK9067 (3) behind the IPTG-inducible promoter P_{spac}. Vancomycin and oxacillin MIC was
 223 determined using Etests in presence or absence of IPTG.

	Vancomycin MIC		Oxacillin MIC	
	no IPTG	IPTG 800µM	no IPTG	IPTG 800µM
JE2pgfp (control)	0.75	0.75	16	16
JE2pvraX	0.75	0.75	12	16
JE2pcwra	0.75	0.75	16	16
JE2pRS02980	0.75	0.75	16	24
JE2pRS08750	0.75	0.75	16	12
JE2psceD	0.75	0.75	16	16
JE2pvraR	0.75	0.75	16	64
JE2pvraS	0.75	0.75	12	16
JE2pvraT	0.75	0.75	12	12
JE2pvraU	0.75	0.75	12	12

224

225

226 **Table S8. Strains used in the study. (16–20)**

Bacterial strains	Description	Source
<i>S. aureus</i> laboratory strains		
JE2	Plasmid-cured derivative of MRSA strain USA300 LAC	16
L1, L2, L3,..., L10	Vancomycin-adapted lineages independently evolved from JE2	This study
L1_E10 to L10_E10	Vancomycin-adapted JE2 clones from 10 rounds of <i>in vitro</i> passaging	This study
L1_E20 to L10_E20	Vancomycin-adapted JE2 clone from 20 rounds of <i>in vitro</i> passaging	Derived from E10 clones This study
L1_E30 to L10_E30	Vancomycin-adapted JE2 clone from 30 rounds of <i>in vitro</i> passaging	Derived from E20 clones This study
N315.1 to N315.5	Vancomycin-adapted N315 clone from 20 rounds of <i>in vitro</i> passaging	This study
110822.1 to 110822.5	Vancomycin-adapted 110822 clone from 20 rounds of <i>in vitro</i> passaging	This study
109384.1 to 109384.5	Vancomycin-adapted 109384 clone from 20 rounds of <i>in vitro</i> passaging	This study
109652.1 to 109652.5	Vancomycin-adapted 109652 clone from 20 rounds of <i>in vitro</i> passaging	This study
110788.1 to 110788.5	Vancomycin-adapted 110788 clone from 20 rounds of <i>in vitro</i> passaging	This study
19902.1 to 19902.5	Vancomycin-adapted 19902 clone from 20 rounds of <i>in vitro</i> passaging	This study
JE2 <i>vraT</i> _{L7_E30}	JE2 with <i>vraT</i> mutation Thr8Met from L7_E30	This study
JE2 <i>vraT</i> _{L8_E20}	JE2 with <i>vraT</i> mutation Ser7Leu from L8_E20	This study
JE2 <i>vraT</i> _{L10_E20}	JE2 with <i>vraT</i> mutation Glu375_Ala377del from L10_E20	This study
JE2 <i>walkK</i> _{L1_E20}	JE2 with <i>walkK</i> mutation Asn335_E336insAspSerPheLeuLeuAspLeuAsn from L1_E20	This study
JE2 <i>walkK</i> _{L7_E20}	JE2 with <i>walkK</i> mutation Ser273Asn from L7_E20	This study
JE2 <i>pgfp</i>	JE2 pSK9067_ <i>gfp</i> - original plasmid carrying the <i>gfp</i> gene behind IPTG-inducible Pspac promoter	This study
JE2 <i>pvraX</i>	JE2 pSK9067_ <i>vraX</i> - plasmid obtained by cloning the <i>vraX</i> gene behind IPTG-inducible P _{spac} promoter	This study
JE2pRS02980	JE2 pSK9067_RS02980 - plasmid obtained by cloning SAUSA300_RS02980 behind IPTG-inducible Pspac promoter	This study
JE2pRS08750	JE2 pSK9067_RS08750 - plasmid obtained by cloning SAUSA300_RS08750 behind IPTG-inducible Pspac promoter	This study
JE2 <i>psceD</i>	JE2 pSK9067_ <i>sceD</i> - plasmid obtained by cloning the <i>sceD</i> gene behind IPTG-inducible Pspac promoter	This study
JE2 <i>pvraR</i>	JE2 pSK9067_ <i>vraR</i> - plasmid obtained by cloning the <i>vraR</i> gene behind IPTG-inducible Pspac promoter	This study
JE2 <i>pvraS</i>	JE2 pSK9067_ <i>vraS</i> - plasmid obtained by cloning the <i>vraS</i> gene behind IPTG-inducible Pspac promoter	This study
JE2 <i>pvraT</i>	JE2 pSK9067_ <i>vraT</i> - plasmid obtained by cloning the <i>vraT</i> gene behind IPTG-inducible Pspac promoter	This study
JE2 <i>pvraU</i>	JE2 pSK9067_ <i>vraU</i> - plasmid obtained by cloning the <i>vraU</i> gene behind IPTG-inducible Pspac promoter	This study
<i>S. aureus</i> clinical isolates		
Mu50	VISA clinical isolate from Japanese hospital in 1996	17
Mu3	hVISA clinical isolate from Japanese hospital in 1996	18
N315	MRSA clinical isolate from Japanese hospital in 1982	19
110822	Clinical isolate	20
109384	Clinical isolate	20
109652	Clinical isolate	20
110788	Clinical isolate	20

228 **Table S9. Assessment of population heterogeneity by sequencing L9 mixed population at**
 229 **E20 and single clone L9_E20.** An aliquot sampled from population L9 at E20 during serial
 230 passaging, and a single clone isolated from this population, were used for genome sequencing.

	Region	Gene	Locus tag	Old locus tag	Type	Reference	Allele	Length	Coverage	Frequency	Average quality	AA change	
L9_E20 single colony	592140	<i>rpoC</i>	SAUSA300_RS02825	SAUSA300_0528	SNV	C	T	1	383	99	33	Arg958Cys	
	610942	/	/	/	SNV	G	A	1	18	100	30		
	721032	<i>vraF</i>	SAUSA300_RS03470	SAUSA300_0647	SNV	C	T	1	89	99	34	Ser55Leu	
	1131799	/	/	/	SNV	T	C	1	75	100	33		
	1959544	/	/	/	SNV	G	T	1	67	100	33		
	2027481	<i>vraT</i>	SAUSA300_RS10195	SAUSA300_1867	SNV	T	C	1	127	99	34	Glu156Gly	
	2027645	<i>vraT</i>	SAUSA300_RS10195	SAUSA300_1867	Deletion	T	-	1	131	94	33	Val102fs	
	2586148	/	SAUSA300_RS13290	SAUSA300_2400	SNV	C	T	1	195	100	34		
	1972154..1972225	<i>prsA</i>	SAUSA300_RS09800	SAUSA300_1790	Deletion			72					Leu204_Glu227del
	1740991	<i>relA</i>	SAUSA300_RS08665	SAUSA300_1590	SNV	G	A	1	128	100	34		<i>Synonymous</i>
L9_E20 population	592140	<i>rpoC</i>	SAUSA300_RS02825	SAUSA300_0528	SNV	C	T	1	345	99	32	Arg958Cys	
	610942	/	/	/	SNV	G	A	1	24	100	36		
	721032	<i>vraF</i>	SAUSA300_RS03470	SAUSA300_0647	SNV	C	T	1	80	100	33	Ser55Leu	
	1131799	/	/	/	SNV	T	C	1	72	99	32		
	1959544	/	/	/	SNV	G	T	1	70	100	32		
	2027481	<i>vraT</i>	SAUSA300_RS10195	SAUSA300_1867	SNV	T	C	1	134	100	34	Glu156Gly	
	2027645	<i>vraT</i>	SAUSA300_RS10195	SAUSA300_1867	Deletion	T	-	1	138	96	34	Val102fs	
	2586148	/	SAUSA300_RS13290	SAUSA300_2400	SNV	C	T	1	182	99	32		
	1972154..1972225	<i>prsA</i>	SAUSA300_RS09800	SAUSA300_1790	Deletion			72					Leu204_Glu227del

231

232

233 **Table S10. Oligonucleotides used in the study.**

Name	Sequence 5'-3'
vraX-FW_Sall	GATACAGTCGACGCAAAGGAGGTAATATAGGTTATG
vraX-RV_EcoRI	GATACAGAATTC TTA ACTA AACTTTTCATATGATCTATATCGTC
cwrA-FW_Sall	GATACAGTCGACATATAAAGGAGTATGATAGCGATGAG
cwrA-RV_EcoRI	GATACAGAATTC TTA AAA GAAATCAGATGGGTAAATTC
RS02980-FW_Sall	GATACAGTCGACAATGTTAGGATGTAATATGTCTTAGAG
RS02980-RV_EcoRI	GATACAGAATTC TCA ATATCCCTCAC TCAATGTAAAC
RS08750-FW_Sall	GATACAGTCGACCATTGGAGGCGAACTATGAG
RS08750-RV_EcoRI	GATACAGAATTCCTATTGATAAGCATTTTCAGATTTTAGTT
sceD-F_Sall	GATACAGTCGACGAGAAACAAATTA CTGTAGGAG
sceD-R_EcoRI	GATACAGAATTC TTATGCAGTAACCCAAATGTCC
vraR-FW_Sall	GATACAGTCGACAATAAGGAGGATTCGTATGACG
vraR-RV_EcoRI	GATACAGAATTCCTATTGAATTAATTTATGTTGGAATGC
vraS-FW_Sall	GATACAGTCGACTATCGGAGACGTAGAGGTG
vraS-RV_EcoRI	GATACAGAATTC TTA ATCGTCATACGAATCCTC
vraT-FW_Sall	GATACAGTCGACATAGAAAGGCGGCGAAAC
vraT-RV_EcoRI	GATACAGAATTC CATCGATAAATCACCTCTACG
vraU-FW_Sall	GATACAGTCGACTAAAAGGTGATAGTTATGAACTATGTTG
vraU-RV_EcoRI	GATACAGAATTCCTATGCCACAGCGTTCA
pSK9067_FW	ATGAACCAAGACAGCATCG
pSK9067_RV	ATGCGTAAGGAGAAAATACCG
walK_L1_L7_FW	CCTCACTAAAGGGAACAAAAGCTGGGTACCATGAAGTGGCTAAAACAAC TAC
walK_L1_L7_RV	CGACTCACTATAGGGCGAATTGGAGCTCTTATTCATCCCAATCACCGTC
vraT_L7_L8_FW	CCTCACTAAAGGGAACAAAAGCTGGGTACCTGTTGCTCAAATTGAGCATA C
vraT_L7_L8_L10_RV	CGACTCACTATAGGGCGAATTGGAGCTCTCATCGATAAATCACCTCTACG
vraT_L10_FW	CCTCACTAAAGGGAACAAAAGCTGGGTACCGCACTACCTTTTAATGCTAGATG

234

235

236 **SI Datasets:**

237

238 **Dataset S1. Mutations from sequencing timepoint E20 and E30 of *in vitro* vancomycin**
239 **evolved strains.** Mutations highlighted in blue were present in E20 and conserved in E30.
240 Mutations highlighted in yellow were present in E20 and lost in E30. Mutations not highlighted are
241 mutations acquired between E20 and E30. (Excel file)

242 **Dataset S2. Feature table for the iModulon structure extracted from the transcriptomic data**
243 **using independent component analysis. ICA yields an activity matrix, which represents the**
244 **activity level of each independent component in each strain, and a weight matrix which**
245 **contains the weight of each gene across each independent component.** (Excel file)

246 **Dataset S3. Expression in E20 strains for selected cell wall and VISA genes.** (Excel file)

247 **Dataset S4. Spearman correlation between gene expression levels and antibiotic MIC. Gene**
248 **expression-antibiotic links are filtered for Spearman $R > 0.7$.** (Excel file)

249 **SI References**

- 250 1. M. Rodriguez de Evgrafov, H. Gumpert, C. Munck, T. T. Thomsen, M. O. A. Sommer,
251 Collateral Resistance and Sensitivity Modulate Evolution of High-Level Resistance to Drug
252 Combination Treatment in *Staphylococcus aureus*. *Molecular Biology and Evolution* **32**,
253 1175–1185 (2015).
- 254 2. I. R. Monk, J. J. Tree, B. P. Howden, T. P. Stinear, T. J. Foster, Complete Bypass of
255 Restriction Systems for Major *Staphylococcus aureus* Lineages. *mBio* **6**, e00308-15.
- 256 3. A. J. Brzoska, N. Firth, Two-Plasmid Vector System for Independently Controlled
257 Expression of Green and Red Fluorescent Fusion Proteins in *Staphylococcus aureus*. *Appl.*
258 *Environ. Microbiol.* **79**, 3133–3136 (2013).
- 259 4. I. R. Monk, T. P. Y. 2021 Stinear, From cloning to mutant in 5 days: rapid allelic exchange in
260 *Staphylococcus aureus*. *Access Microbiology* **3**, 000193.
- 261 5. F. Radicchi, C. Castellano, F. Cecconi, V. Loreto, D. Parisi, Defining and identifying
262 communities in networks. *PNAS* **101**, 2658–2663 (2004).
- 263 6. A. V. Sastry, *et al.*, The *Escherichia coli* transcriptome mostly consists of independently
264 regulated modules. *Nat Commun* **10**, 5536 (2019).
- 265 7. S. Poudel, *et al.*, Revealing 29 sets of independently modulated genes in *Staphylococcus*
266 *aureus*, their regulators, and role in key physiological response. *Proc Natl Acad Sci U S A*
267 **117**, 17228–17239 (2020).
- 268 8. R. B. D'Agostino, A. Belanger, A Suggestion for Using Powerful and Informative Tests of
269 Normality. *The American Statistician* **44**, 316–321 (1990).
- 270 9. F. Pedregosa, *et al.*, Scikit-learn: Machine Learning in Python. *J. Mach. Learn. Res.* **12**,
271 2825–2830 (2011).
- 272 10. S. Boyle-Vavra, S. Yin, D. S. Jo, C. P. Montgomery, R. S. Daum, *VraT/YvqF* Is Required for
273 Methicillin Resistance and Activation of the *VraSR* Regulon in *Staphylococcus aureus*.
274 *Antimicrob Agents Chemother* **57**, 83–95 (2013).
- 275 11. A. Delauné, *et al.*, The WalkR System Controls Major Staphylococcal Virulence Genes and
276 Is Involved in Triggering the Host Inflammatory Response. *Infect Immun* **80**, 3438–3453
277 (2012).
- 278 12. D. A. Ravcheev, *et al.*, Inference of the transcriptional regulatory network in *Staphylococcus*
279 *aureus* by integration of experimental and genomics-based evidence. *J Bacteriol* **193**,
280 3228–3240 (2011).
- 281 13. M. Kuroda, *et al.*, Two-component system *VraSR* positively modulates the regulation of cell-
282 wall biosynthesis pathway in *Staphylococcus aureus*. *Molecular Microbiology* **49**, 807–821
283 (2003).
- 284 14. M. Falord, U. Mäder, A. Hiron, M. Débarbouillé, T. Msadek, Investigation of the
285 *Staphylococcus aureus* GraSR Regulon Reveals Novel Links to Virulence, Stress
286 Response and Cell Wall Signal Transduction Pathways. *PLoS One* **6** (2011).
- 287 15. A. Rajput, *et al.*, Pangenome Analytics Reveal Two-Component Systems as Conserved
288 Targets in ESKAPEE Pathogens. *mSystems* **6** (2021).

- 289 16. P. D. Fey, *et al.*, A Genetic Resource for Rapid and Comprehensive Phenotype Screening
290 of Nonessential *Staphylococcus aureus* Genes. *mBio* **4**, e00537-12 (2013).
- 291 17. K. Hiramatsu, *et al.*, Methicillin-resistant *Staphylococcus aureus* clinical strain with reduced
292 vancomycin susceptibility. *J Antimicrob Chemother* **40**, 135–136 (1997).
- 293 18. K. Hiramatsu, *et al.*, Dissemination in Japanese hospitals of strains of *Staphylococcus*
294 *aureus* heterogeneously resistant to vancomycin. *The Lancet* **350**, 1670–1673 (1997).
- 295 19. K. Okonogi, Y. Noji, M. Kondo, A. Imada, T. Yokota, Emergence of methicillin-resistant
296 clones from cephamycin-resistant *Staphylococcus aureus*. *J Antimicrob Chemother* **24**,
297 637–645 (1989).
- 298 20. K. Mikkelsen, “Intrinsic resistance mechanisms and CRISPR-Cas immunity of the
299 opportunistic pathogen, *Staphylococcus aureus*.” PhD thesis (2021).
- 300